Proceedings of Meetings on Acoustics

Volume 26 http://acousticalsociety.org/

171st Meeting of the Acoustical Society of America

Salt Lake City, Utah
23-27 May 2016

Engineering Acoustics: Paper 2pEA8

Recording anechoic gunshot waveforms of several firearms at 500 kilohertz sampling rate

Tushar K. Routh and Robert C. Maher
Department of Electrical and Computer Engineering, College of Engineering, Montana State University, Bozeman, Montana; tusharrouth@gmail.com , rob.maher@montana.edu

Acoustic gunshot signals consist of a high amplitude and short duration impulsive sound known as the muzzle blast and the shock wave. This experiment involved documenting gunshot muzzle blast sounds produced by eight commonly used firearms including Remington 870, Colt 45, Glock 19 with 9mm ammunition, Glock 23, Sig 239, AR15, 22LR, and Ruger SP 101 with 357 magnum and 38 special ammunition. An elevated microphone bracket (3m above the ground) was built to achieve a quasi-anechoic environment for the duration of the muzzle blast. Twelve microphones (GRAS 40DP) were mounted on the bracket in a semi-circular arc to observe the azimuthal variation of the muzzle blast. Signals were recorded using LabVIEW. Similarities and differences among waveforms are presented.

Published by the Acoustical Society of America

 [DOI: 10.1121/2.0000262]

INTRODUCTION

Recorded gunshot signals consist of two major waveforms of interests, the muzzle blast, originated from the rapid combustion of gunpowder, and the ballistic shock wave produced by the bullet if traveling at supersonic speed (Maher, 2013). If analyzed carefully, these waveforms can provide information about the shot type, directionality and some other significant facts. Real life muzzle blasts and shock wave signals are brief in duration, spanning less than a few milliseconds, so capturing these brief acoustic waveforms requires a high sampling rate. In addition to the direct sound path, the muzzle blast and ballistic shock sounds are also reflected from nearby surfaces and from the ground, which results in a complicated received signal at the measurement position. In this experiment, we recorded gunshot signals from several common firearms in a quasi-anechoic manner with a sampling rate of 500 kHz. A number of successive shots were recorded for each firearm type. A relative comparison of the signal characteristics is presented.

METHODOLOGY

The experiment for gunshot sound recording was executed outdoors at a ranch near Bozeman, Montana, on October 14, 2015. Our primary goal was to observe gunshot signal variation as a function of azimuth for several types of firearms. A total of twelve microphones were placed near the shot in a semicircular arc covering 180 degrees relative to the direction of the fired shot. Distances from each microphone to the shooting position were assumed to be nearly equal and the semicircular microphone frame was held constant throughout the experiment.

Gunshot signals are known to be affected by reflections from the surrounding structures and also from the ground. If the time differences between the direct and reflected waves are not maintained properly, interference between the direct and reflected sounds makes the captured signals difficult to interpret. To overcome this issue, the shooter and the semicircular array of twelve microphones was elevated 3 m above the ground, as shown in Figure 1. Due to the open air environment, it could be assumed that the first reflected waves would come from ground reflection. The path length difference provided by the elevated shooting position and microphones caused the ground reflected waves to appear at the microphones nearly 10 milliseconds after the direct sound arrival, providing a quasi-anechoic recording of the muzzle blast and shock wave (Maher and Routh, 2015).

Figure 1: Shooting from an elevated platform to create time lag between the direct and ground-reflected signals

A. Recording System

Microphones with small diaphragm diameters are well suited for measuring signals with high frequency and amplitude such as gunshot blasts. The recording microphones used in this experiment were G.R.A.S. 40DP (diameter = 0.125 inches) condenser microphones (Figure 2(a)). These condenser microphones are externally polarized with rear venting features. The 40DP capsules are suitable for conducting gunshot blast recordings because of their relatively low sensitivity (0.68 mV/Pa to 0.9 mV/Pa in this experiment), wide frequency response (flat response from 6.5 Hz to nearly 70 kHz), and wide dynamic range (from 40 dB to 175 dB). The microphones were calibrated using a G.R.A.S. type 42AB calibrator at 250 Hz (114 dB SPL with reference to 20µPa).

Among the twelve microphones, the first eight were connected to a G.R.A.S. 12AG 8-Channel Power Module (Figure 2(b)). They provided the flexibility to carry out experiment either from a mains/line supply or from an external DC supply (12 V – 18 V). To capture the whole range of amplitude, 20dB attenuators were connected on the output side of each channel. The rest of the four microphones were connected to two G.R.A.S. 12AA 2-Channel Power Modules which were equipped with built-in attenuation range of -20dB to +40dB (Figure 2(c)).

(a)

(b)

(c)

Figure 2: (a): G.R.A.S. 40 DP Microphone capsule;
(b) G.R.A.S. 12AG 8-channel Module;
(c) G.R.A.S. 12AA Module

Amplifier outputs were then connected to a Multichannel Data Acquisition System developed by National Instruments (NI). The NI PXIe-1071 PXI express chassis was used along with a NI PXIe-6358 data acquisition device (DAQ). This multifunction system supports 16 simultaneous analog inputs at 1.25 MS/s/channel with 16-bit resolution. For our analysis requiring 12 channels, we used eight channels on one slot and four on the other.

Signals were gathered using a custom program implemented with LABVIEW. Twelve separate channels were recorded simultaneously at a sampling rate of 500 kilohertz per channel. It was expected that this high sampling rate would enable sensors to capture high pressure peaks occurring over a brief duration. The acquisition mode was set to differential and the differential voltage range was specified between +5V to -5V. Following acquisition, each signal was imported into MATLAB for additional analysis.

B. Microphone Orientation

The first of the twelve microphones was aligned directly in the line of fire and the other microphones were spaced equally in azimuth up to 180 degrees (~16 degree angular spacing). Microphone holders of various lengths were made and connected to the straight segments of the metal frame to keep the distance from the shooting position to each sensor equal. The sensitivities of different microphones are given in Table 1.

Table 1: Measured sensitivities of twelve G.R.A.S. 40DP microphones

Microphone	Sensitivity (in mV/Pa)	Microphone	Sensitivity (in mV/Pa)
01	0.90	07	0.90
02	0.68	08	0.84
03	0.85	09	0.91
04	0.88	10	0.75
05	0.84	11	0.84
06	0.69	12	0.82

Angular positions of the microphones relative to the line of fire are shown in Figure 3.

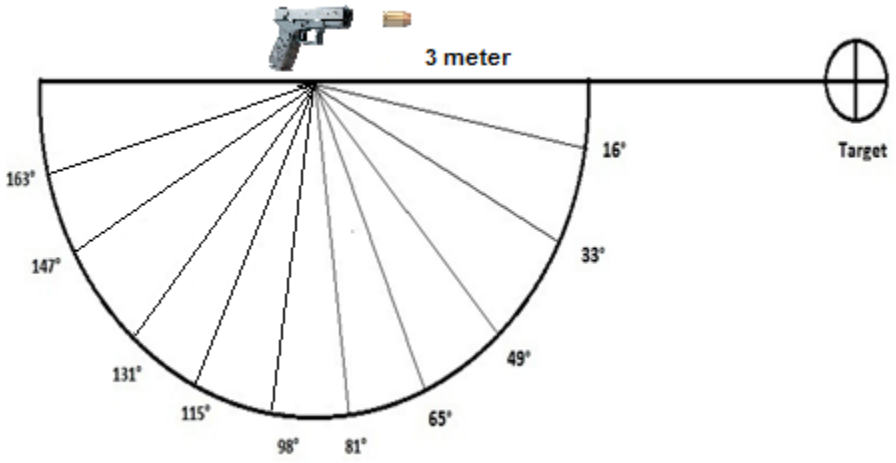

Figure3: Microphone azimuths relative to the line of fire

C. Firearm Types

To cover a wide range of commonly used firearms, our experiment tested ten different firearms including shotgun, pistol, revolver, and rifle. Parameter variations in the tested firearms can be seen below in Table 2.

Table 2: List of firearms and ammunition for this experiment

Firearm	Type	Ammunition	No. of shots observed
Remington 870	Shotgun	12 gauge 3 inch	3
CZ 452	Rifle	22 LR	10
Surgeon / AI	Rifle	308 Winchester	10
Colt 1911	Pistol	45 ACP	10
Glock 19	Pistol	9x19	10
Glock 23	Pistol	40 S&W	10
Sig 239	Pistol	357 Sig	10
Ruger SP101	Revolver	357 Magnum	9
Ruger SP101	Revolver	38 Special	10
Stag Arms AR15	Rifle	5.56 NATO	10

ACOUSTIC FEATURES OBSERVED

The goals of this experiment were:

- To observe the azimuthal variation of each shot.
- To compare the acoustical features from one firearm and ammunition combination to the other.

To typify a particular shot, the observed features are

- Peak acoustic pressure at a particular azimuth
- Muzzle blast duration
- Total acoustic energy emission from a shot

For the purposes of this paper we have chosen the AR-15 semi-automatic rifle as the primary demonstration example. This firearm produces both the muzzle blast and the ballistic shock wave characteristics.

RESULTS AND DISCUSSION

The gunshot acoustical signal shows significant difference as a function of azimuth. The ballistic shock wave is visible for the small azimuth angles, but with different amplitude and time-of-arrival due to the geometry of the shock wave disturbance (Maher, 2013). For example, AR15 was fired with the bullet XM855 62 gr, Lake City 2014, which had a velocity of approximately 3100 feet per second (945 m/s). This provides a Mach number equal to 2.8 and a Mach angle 20.8°. As the bullet travels downrange in the line of fire, the shockwave travels outwards as a cone with interior aspect equal to the Mach angle. So the time difference between the shock wave and the muzzle blast decreases with increasing azimuth angle, and is not observed at higher azimuths where the shock wave from the bullet's trajectory does

not propagate. Figure 4 summarizes the azimuthal gunshot waveform variation for the AR15. Peak pressure levels (in Pascal) have been plotted against time (in milliseconds).

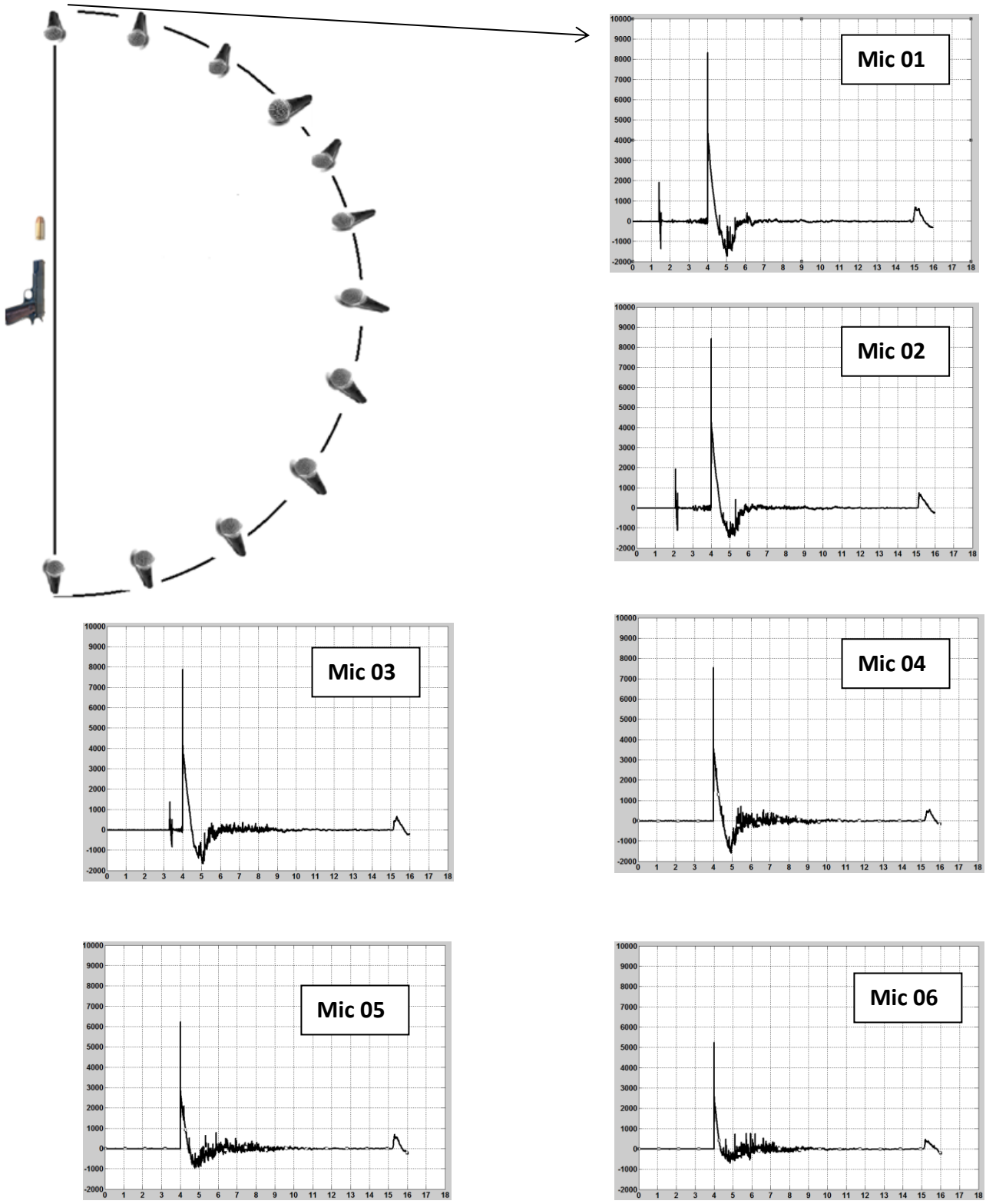

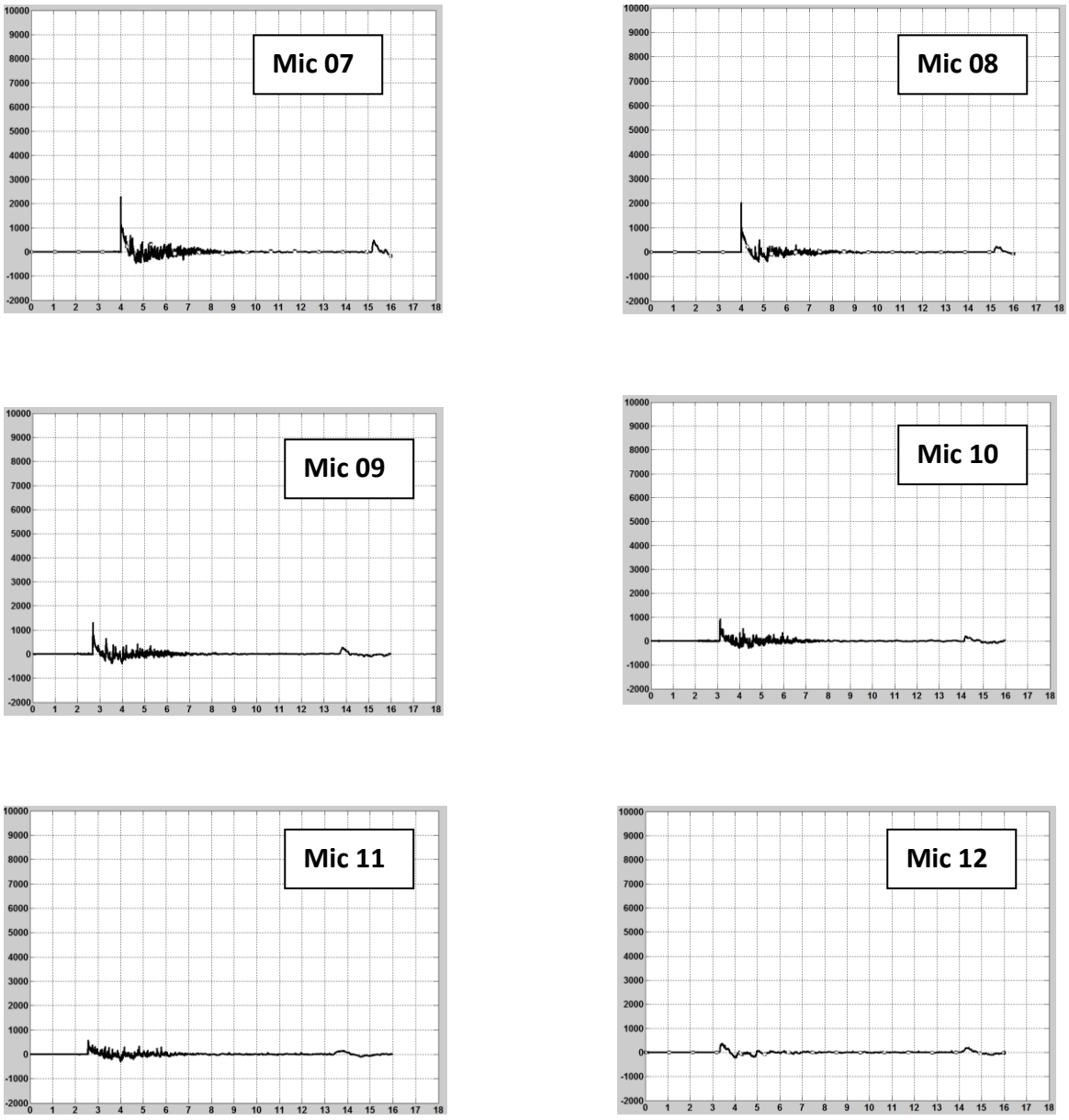

Figure 4: Azimuthal variation of AR 15 (with bullet XM855 62 gr, Lake City 2014)

A. Peak Pressure variation

Peak pressure was recorded for a number of shots at different azimuths. Figure 5 and Figure 6 exhibit azimuthal peak pressure variation and shot-to-shot peak pressure variation in the line of fire (microphone 1) for the AR15.

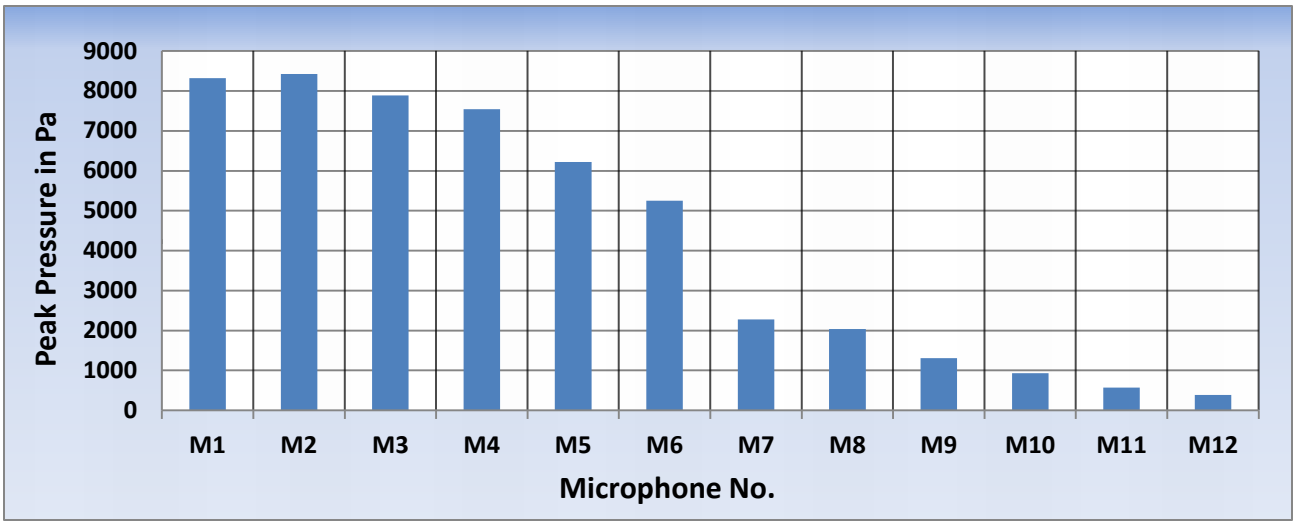

Figure 5: Peak pressure variation for the first shot of AR15 as a function of azimuth

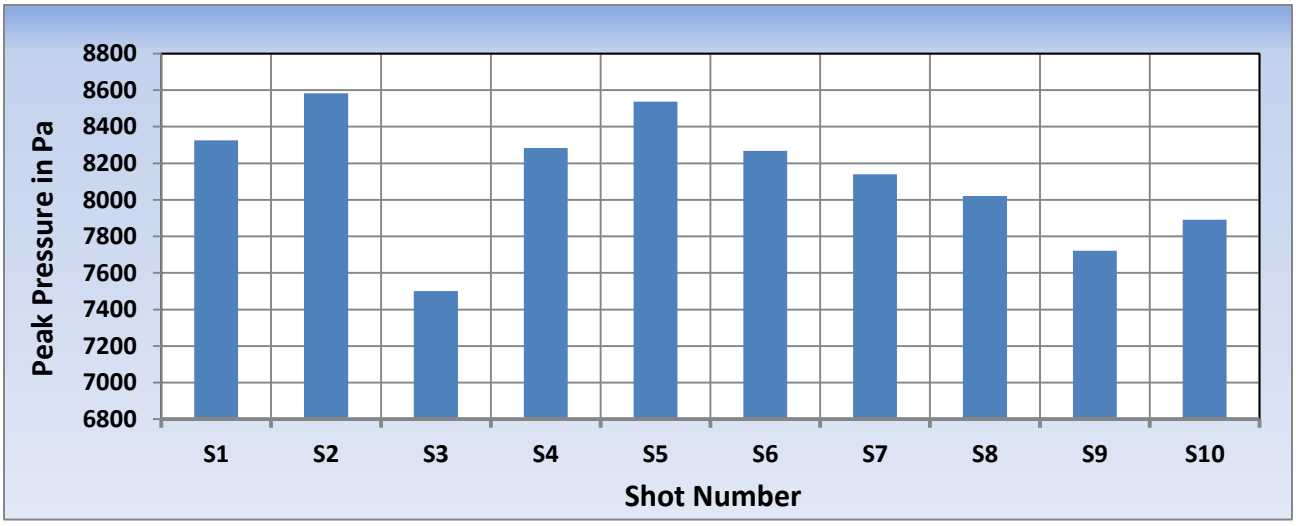

Figure 6: Shot to shot peak pressure variation on-axis (microphone 1) for successive shots for AR15 at the line of fire

AR15 rifles are long barrel weapons. The inside of the barrel is grooved (rifled) into a helical shape to generate more accuracy and speed toward the target, and also a very high peak pressure as shown in Figure 5. The variation in peak pressure (Figure 6) from one shot to another may be due to a change in position of the hand-held firearm during the experiment or possibly a variation from one cartridge to another in the unmatched set of commercial ammunition used.

B. Muzzle Blast Duration Variation

Hot expanding gas exits the barrel as the bullet is expelled. Due to the momentary over-pressure in the vicinity of the muzzle, and the acoustic impedance mismatch between the barrel and the air, progressive waves move outward and reflected waves move back and forth in the barrel. As a result, in spite of getting a single point peak, the muzzle blast pressure waveform extends until the disturbance settles down (Rasmussen, Flamme, Stewart, Meinke, & Lankford, 2010). We calculate the overall positive and negative pressure duration as the muzzle blast duration.

In this paper, the muzzle blast duration was calculated by adding up the time that the blast signal stays above the mean value of the total signal (the *positive phase duration*) and the time the signal remains below the mean value and returns to the mean (the *negative phase duration*). With the increase of azimuth from the line of fire, the pressure amplitude decreases, and it may become difficult to interpret the duration with good precision. The azimuthal variation of muzzle blast is shown in Figure 7.

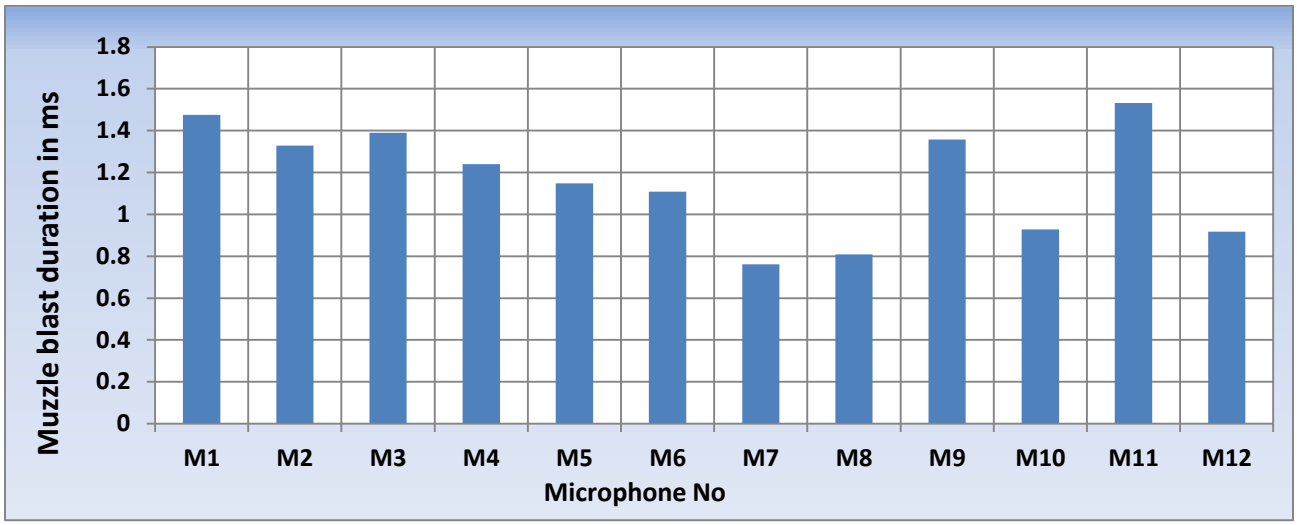

Figure 7: Azimuthal variation of muzzle blast durations for AR15

C. Acoustical energy accumulation on-axis

To have a closer look at the muzzle blast acoustic energy accumulation of the AR15, we have selected the muzzle blast portion (in this case, 5 milliseconds) as shown in Figure 8. Figure 9 shows how the energy accumulates from the beginning to end. Figure 10 shows an enlarged version of Figure 9.

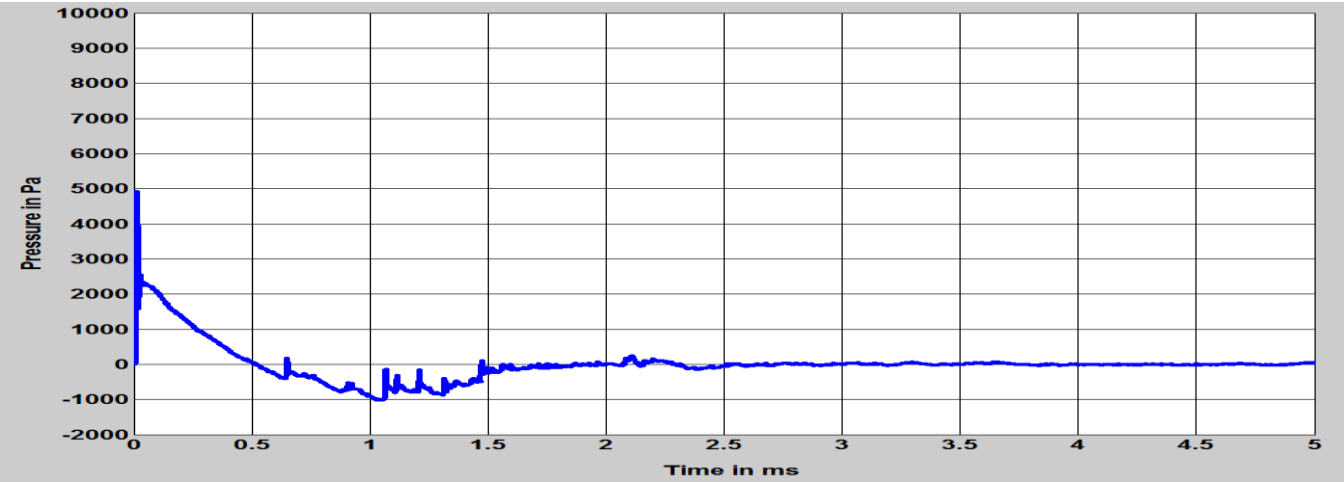

Figure 8: Muzzle blast portion of AR15 (Shot 01, Mic01)

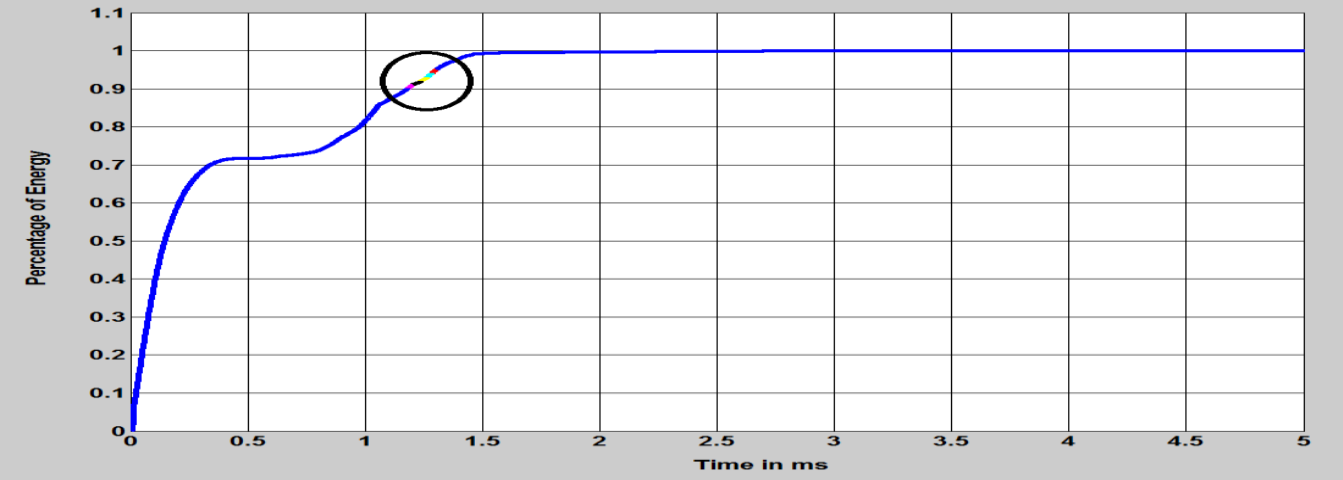

Figure 9: Energy accumulation during the muzzle blast

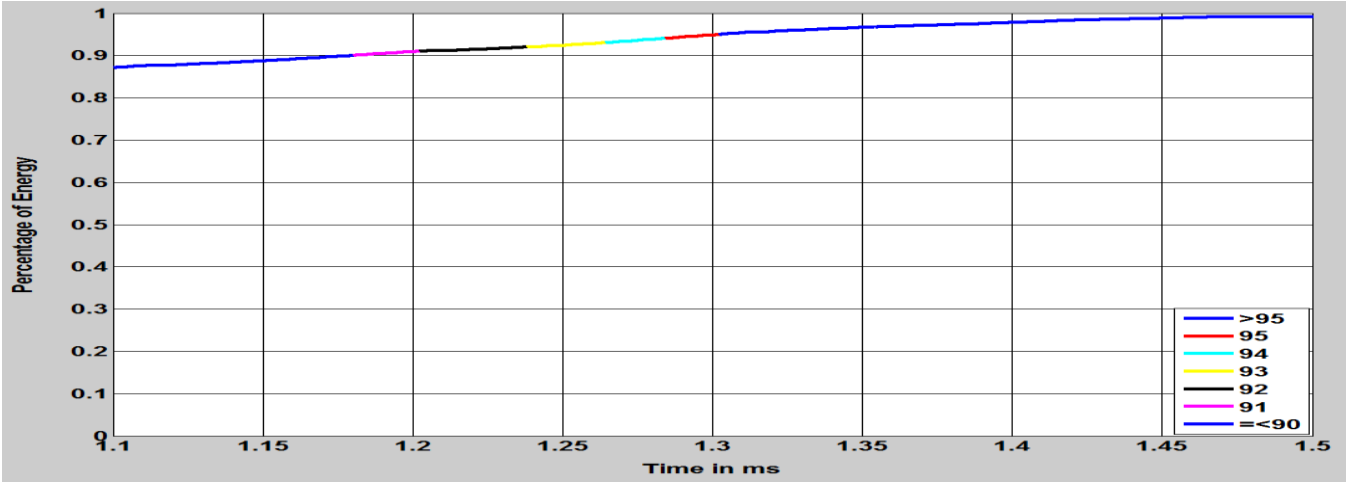

Figure 10: Enlarged view of energy accumulation (circled portion of Figure 9)

Energy here is calculated by taking the square of the microphone voltage at each point (i.e., acoustical energy is proportional to pressure squared). If we take a closer look at Figure 9, there is a sudden rise of energy at the start, as there is a sudden rise of pressure during that portion. There is a plateau region immediately after that as the pressure values return momentarily to near the average value. Then the energy again creeps up during the negative pressure portion. The percentages of interest are all clustered at this portion. After a sufficient time the energy accumulation approaches its total and the rest of the samples have little additional energy to contribute to the total.

D. Total energy of a shot

In general, the energy from the muzzle blast expands in all directions as depicted in Figure 11. Thus, the total acoustical energy calculation needs to be three dimensional, and take into account the azimuthal differences in the acoustical signal.

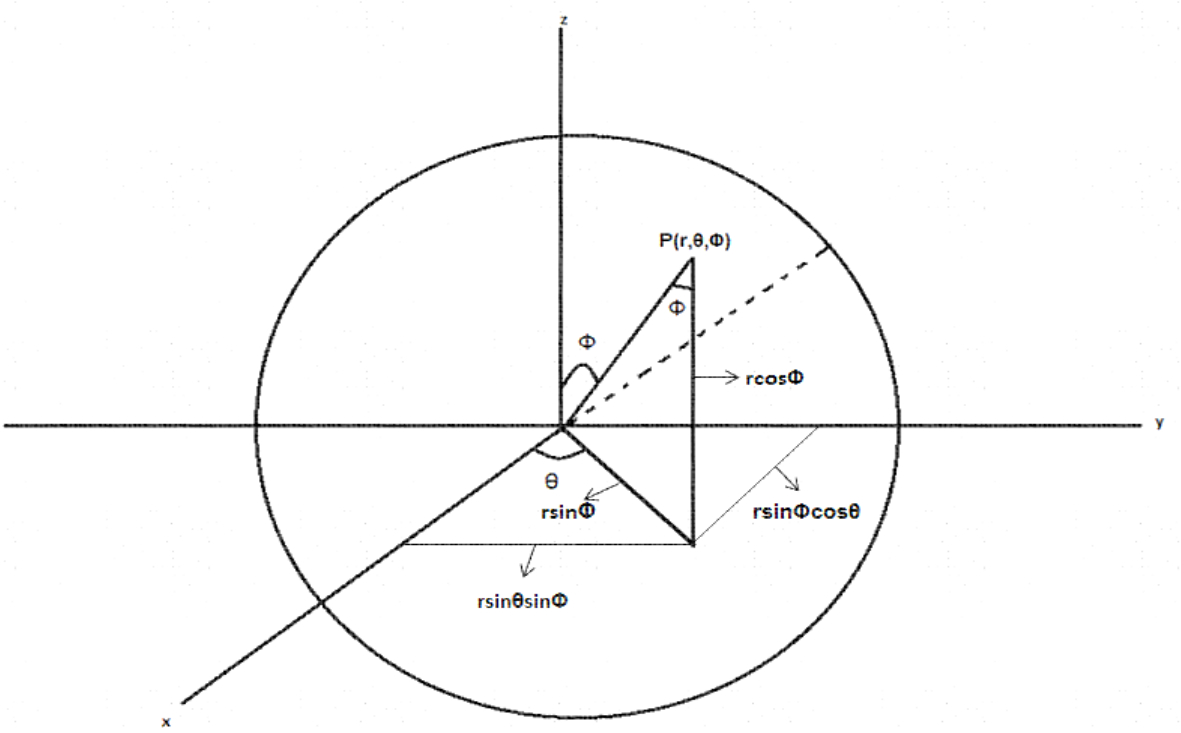

Figure 11: Geometry of muzzle blast acoustical energy propagation in three dimensions

In our case, all our microphones were set at a fixed distance r=R=3 meters. As our observation suggests, the energy distribution is not purely spherical, and varies at different azimuths.

$$E_{total} = \frac{2\pi R^2}{\rho_0 c} \sum P^2(\theta) sin\theta d\theta$$

It is assumed that the pressure values are symmetrical cylindrically with respect to the line of fire. Figure 12 summarizes the variation of energy calculated for each of ten successive shots for the AR15. The shot-to-shot variation may be due to the imprecise position of the hand-held firearm and possibly cartridge-to-cartridge differences in the commercial ammunition used for these tests.

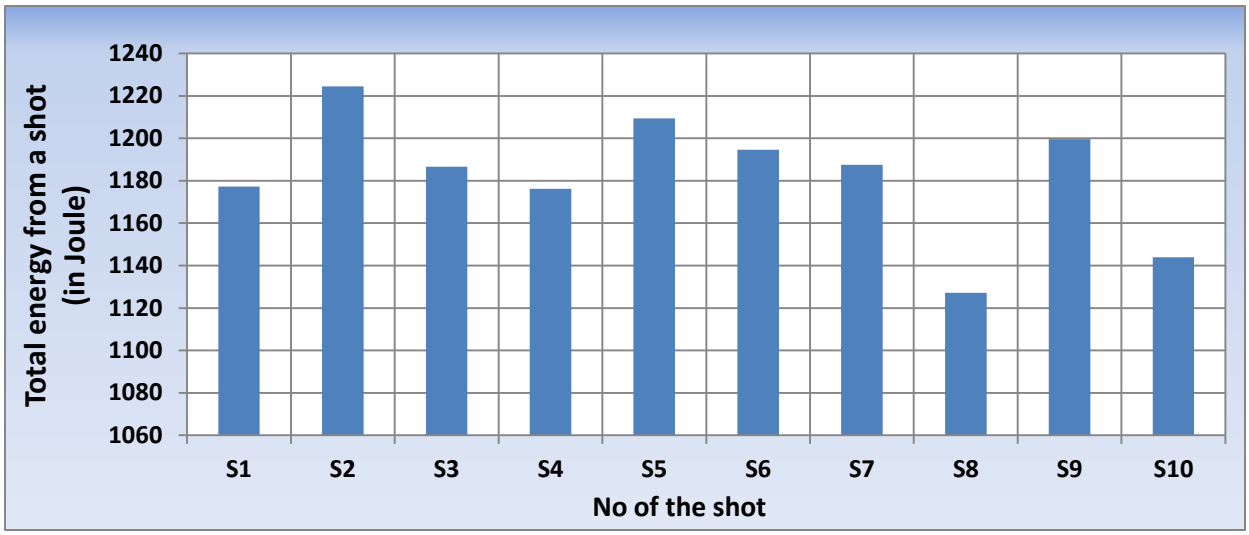

Figure 12: Variation of total energy emission of AR 15

E. Comparison between firearms

Figure 13 shows the peak pressure variation of the different firearms. The data are taken from the first shot with each gun as measured by the on-axis microphone (microphone 1). The lowest peak pressure was for the 0.22 caliber rifle (22LR), as it was the smallest caliber tested, and also the only firearm where the bullet was rim fire rather than centerfire. As expected, the rifles score the highest pressure according to their internal ballistics. Two Glock handguns generate different pressure values because of their bullet type: the Glock 19 was fired with 135 gr Hornady bullet whereas Glock 23 was equipped with 165 gr Remington. The Sig 239 and Glock 19 handguns show a substantial difference between the maximum and minimum peak pressure, perhaps caused by imprecise positioning of the firearm during a particular shot. Although the shotgun (12 gauges) level is comparable to the rifles, the sound characteristics are different in timing and wave shape.

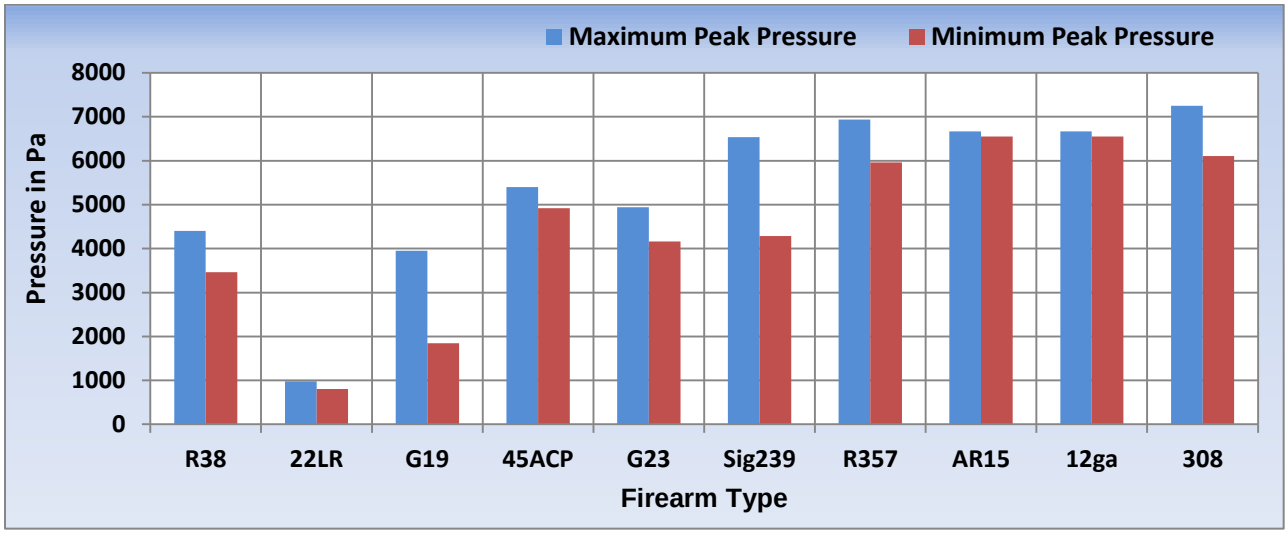

Figure 13: Peak Pressure variation of different firearms

Muzzle blast duration variations of different firearms are also observed. 12ga shotgun takes the highest time to resettle to mean pressure. There is again a noticeable difference between similar firearm having different ammunitions.

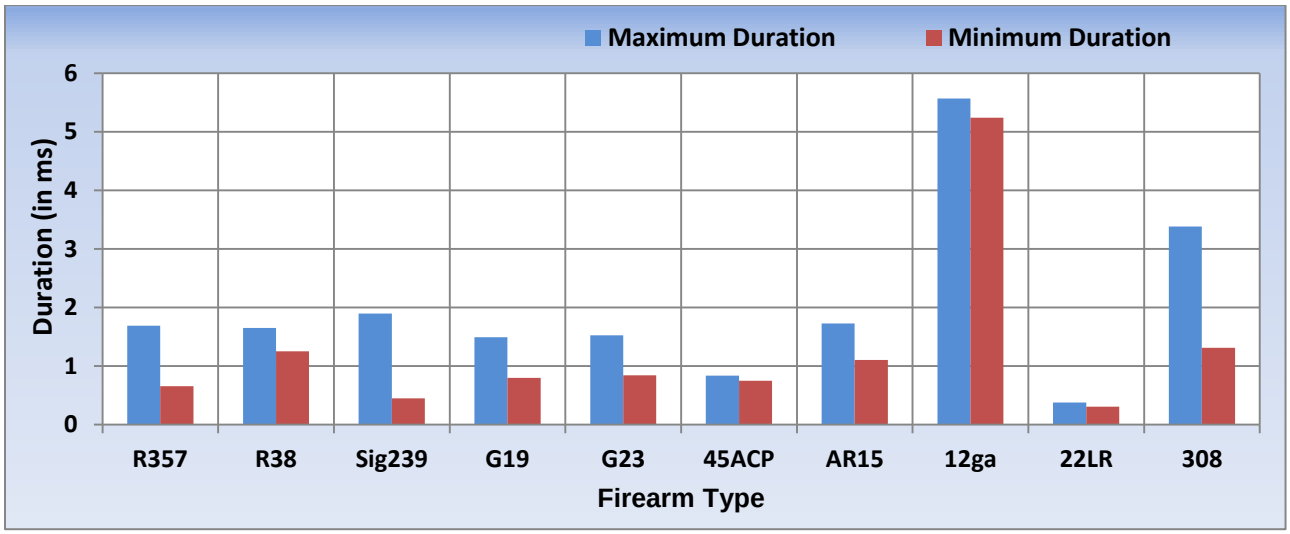

Figure 14: Muzzle blast duration variation in different firearms

Total energy emission variation was also observed. As this energy calculation is based upon a time integral of the squared pressure response, this graph is similar to the pressure curve.

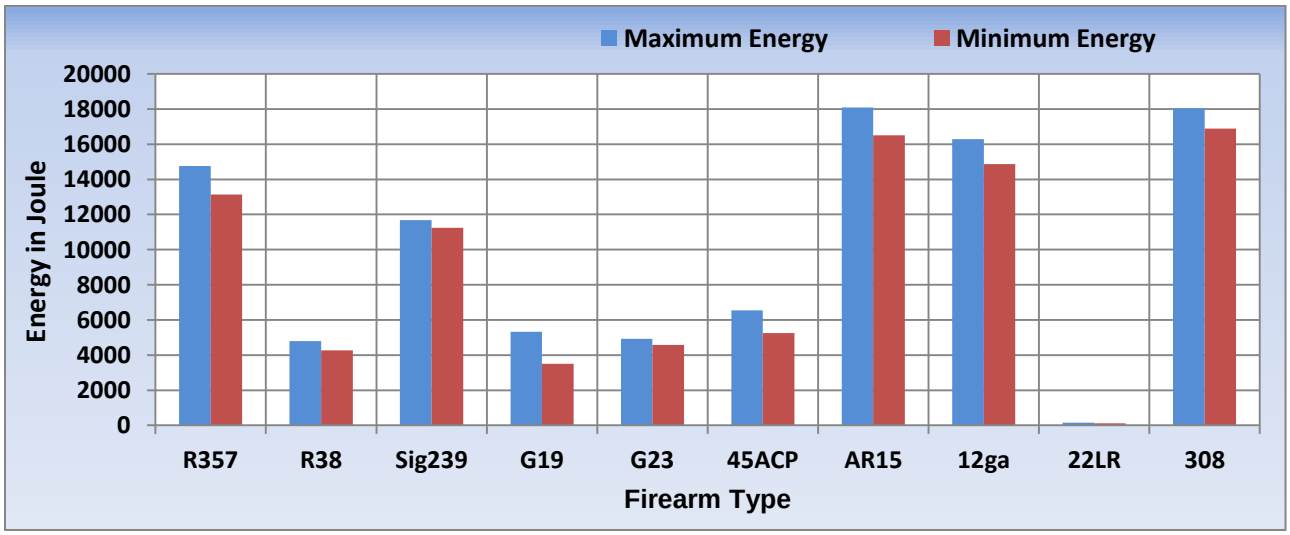

Figure 15: Total energy variation of different firearms

CONCLUSIONS

Acoustic gunshot signals exhibit significant variation according to the azimuth. As seen, there are also variations from one shot to another for the same ammunition. There can be several reasons behind that. In this experiment, simultaneous shots were not targeted at the same point. Moreover, variations in internal ballistics of the bullets can also lead these discrepancies. In future, our plan is to take account of these facts. Our effort will be to model the acoustic signature at particular azimuths and for different firearms. Moreover, as seen, the behavior of a single firearm differs from one kind of bullet to another; our future endeavor will also include taking a closer look at these variations.

ACKNOWLEDGEMENTS

Our research results work is supported by the National Institute of Justice (Award: 2014-DN-BX-K034) for Research and Development in Forensic Science for Criminal Justice Purposes. We are also grateful to Dr. Steven Shaw, Professor, Electrical & Computer Engineering, Montana State University and Angelo Borzino, Lieutenant Colonel, Military Engineering Institute, Rio de Janeiro, Brazil, for their assistance with our gunshot recordings and interpretation.

REFERENCES

Maher, Robert C. (2013). Acoustical characterization of Gunshots, IEEE, pp. 1–5. Available: http://ieeexplore.ieee.org/xpls/abs_all.jsp?arnumber=4218954.

Maher, Robert C. & Routh, T. K. (2015). Advancing Forensic Analysis of Gunshot Recordings. In Audio Engineering Society Convention 131 (pp. 1–8). New York.

Rasmussen, P., Flamme, G., Stewart, M., Meinke, D., & Lankford, J. (2010). Measuring recreational firearm noise. The Journal of the Acoustical Society of America, 127(3), 1794. http://doi.org/10.1121/1.3384002